

Detection of gravitational waves from the QCD phase transition with pulsar timing arrays

Chiara Caprini¹, Ruth Durrer² and Xavier Siemens³

²*CEA, IPhT & CNRS, URA 2306, F-91191 Gif-sur-Yvette, France*

²*Département de Physique Théorique, Université de Genève*

24 quai Ernest Ansermet, CH-1211 Genève 4, Switzerland

³*Center for Gravitation and Cosmology, Department of Physics, University of Wisconsin–Milwaukee
P.O. Box 413, Milwaukee, Wisconsin 53201, USA*

(Dated: February 5, 2022)

If the cosmological QCD phase transition is strongly first order and lasts sufficiently long, it generates a background of gravitational waves which may be detected via pulsar timing experiments. We estimate the amplitude and the spectral shape of such a background and we discuss its detectability prospects.

PACS numbers: 98.80.-k, 25.75.Nq, 04.30.Db, 04.80.Nn

I. INTRODUCTION

Gravitational waves (GWs) are space-time fluctuations that propagate at the speed of light through empty space; they were predicted by Einstein in 1916 [1]. Because of the weakness of the gravitational interaction, GWs could provide information about astrophysics and cosmology from regions and epochs of the Universe from which electromagnetic radiation cannot propagate freely. For the same reason, however, GWs have thus far eluded direct detection, despite considerable efforts.

Advanced configurations of existing ground-based interferometers such as LIGO [2] and VIRGO [3] are expected to detect GWs in the next years. Terrestrial interferometers have best sensitivity at a frequency $f \sim 100$ Hz, and are severely limited by seismic noise below a few Hertz. GWs with significantly lower frequency, $f \sim 10^{-9}$ Hz, are also expected to be detected by pulsar timing experiments in the next decade [4, 5]. A worldwide collaboration of astronomers, the International Pulsar Timing Array (IPTA) project [4], has been formed with the goal of detecting nano-Hz GWs using millisecond pulsars. Millisecond pulsars are rapidly rotating, highly magnetized neutron stars which emit a beam of electromagnetic radiation that sweeps over the earth once per rotation. They constitute extremely accurate clocks that could be used to detect GWs. Candidates for the generation of a GW background in the nano-Hz band are super-massive black hole binary mergers [6–11] and cosmic strings [12–16].

In this paper we study another potential candidate: the cosmological QCD phase transition, which is believed to have taken place when the Universe had a temperature of $T_* \simeq 100$ MeV. A GW background can be generated by the QCD phase transition if it is first order, and the characteristic frequency of this background falls in the frequency band of pulsar timing experiments. We show here that, if the phase transition is sufficiently strong and lasts for a sufficiently long time, the GWs produced can be observed in future pulsar timing experiments. This possibility has been discussed for the first time by Wit-

ten in Ref. [17]. Here we present accurate predictions for the spectrum of the emitted gravitational radiation as a function of the phase transition parameters like its temperature, strength and duration.

In the context of standard cosmology and QCD, the cosmological QCD phase transition is not even second order but a cross-over, and we do not expect it to generate GWs. However, if the neutrino chemical potential is sufficiently large (still well within the bounds allowed by big bang nucleosynthesis), it can become first order [18]. Furthermore, if a sterile neutrino is the dark matter, we do expect a large neutrino chemical potential [19].

Thus, pulsar timing experiments could open a new cosmological window: the detection of a stochastic background of GWs could help to determine whether the QCD phase transition is first order. The amplitude and peak frequency of the spectrum are also sensitive to the expansion rate of the Universe during this phase transition [20], which is currently unconstrained.

In the next section we provide estimates for the GW spectrum by a first order QCD phase transition. In Section III we compare our results with current and expected sensitivities of pulsar timing arrays. We conclude in Section IV. Throughout we use the metric signature $(-, +, +, +)$ and conformal time so that the Friedmann metric is given by $ds^2 = a^2(t)(-dt^2 + d\mathbf{x}^2)$. The conformal Hubble parameter is denoted by $\mathcal{H} = \dot{a}/a = Ha$. An over-dot denotes the derivative w.r.t conformal time t .

II. GRAVITATIONAL WAVES FROM A FIRST ORDER QCD PHASE TRANSITION

Very violent processes in the early universe can lead to the generation of GWs. One example of such violent processes are first order phase transitions [17, 21–24], which can lead to GW production via the collision of bubbles of the true vacuum [25–33] and via the turbulence and magnetic fields they can induce in the cosmic plasma [34–41].

The GWs generated by a source are determined by the linearized Einstein equation for tensor perturbations in a

Friedmann background [42],

$$\ddot{h}_{\pm} + 2\frac{\dot{a}}{a}\dot{h}_{\pm} + k^2 h_{\pm} = 8\pi G a^2 \rho \Pi_{\pm}. \quad (1)$$

Here ρ is the background cosmological energy density, a is the scale factor, Π_{\pm} are the two tensor helicity modes of the (dimensionless) anisotropic stress which is the source of GWs, and h_{\pm} are the helicity modes of the GW. If an anisotropic stress is generated at some time t_* in the radiation dominated era, from a source with relative energy density $\Omega_{S^*} = \rho_{S^*}/\rho_*$, we expect Π to be at best of the order of Ω_{S^*} . The GW energy density (from two polarizations \pm which contribute equally) is given by

$$\rho_{\text{GW}}(t) = \frac{\langle \dot{h}_{+}(\mathbf{x}, t) \dot{h}_{+}(\mathbf{x}, t) \rangle}{8\pi G a^2(t)}. \quad (2)$$

Due to statistical homogeneity, ρ_{GW} is independent of the position. The GW energy spectrum per logarithmic unit of frequency $\frac{d\rho_{\text{GW}}(k, t)}{d\log(k)}$ is defined by

$$\rho_{\text{GW}} = \int \frac{dk}{k} \frac{d\rho_{\text{GW}}(k, t)}{d\log(k)}.$$

Detailed semi-analytical and numerical calculations have been performed in the past in order to calculate the GW energy spectrum from first order phase transitions [25–41]. In this paper we simply use analytic fits to the most recent results, as presented in the following.

Concerning the GW signal from bubble collisions, we use the shape of the spectrum proposed in Ref. [33], but rescale the amplitude to agree with the numerical result of Ref. [31]. As a result, the GW energy density emitted by this source is well approximated by

Bubble collisions:

$$\frac{d\Omega_{\text{GW}}^{(\text{B})} h^2}{d\log k} \simeq \frac{2}{3\pi^2} h^2 \Omega_{r0} \left(\frac{\mathcal{H}_*}{\beta} \right)^2 \Omega_{S^*}^2 v^3 \frac{(k/\beta)^3}{1 + (k/\beta)^4}. \quad (3)$$

Here Ω_{r0} denotes the radiation energy density today, $h = H_0/(100\text{km/s/Mpc})$ is the present Hubble parameter in units of 100km/s/Mpc, β^{-1} is the duration of the phase transition, v is the expansion velocity of the bubbles, and k is the co-moving wave-number or frequency of the GW. The GW spectrum is proportional to the relative energy density in the source $\Omega_{S^*}^2$, to the ratio between the duration of the phase transition and the Hubble time $(\mathcal{H}_*/\beta)^2$, and to the bubble velocity v^3 [31].

The QCD phase transition is expected to happen at the temperature $T_* \simeq 100$ MeV, when the kinetic and magnetic Reynolds numbers of the cosmic fluid are very large [41]. The bubbles which rapidly expand and collide are therefore expected to generate magnetohydrodynamical (MHD) turbulence in the cosmic fluid. The kinetic energy of the turbulent motions and the magnetic fields sustained by the MHD turbulence also induce

GWs: Ref. [41] presents the latest semi-analytical calculation of the GW spectrum from MHD turbulence. There are two important differences with respect to the GW signal from bubbles. First, turbulence lasts beyond the duration of the phase transition: this leads to an enhancement of the signal on large (super-horizon) scales [41]. Second, the time correlation properties of the anisotropic stress source are different. For bubble collisions, the source is totally coherent (see [33, 41]), while for MHD turbulence the source is coherent only over about one characteristic wavelength [41]. This leads to a difference in the peak position of the GWs from the two sources: while the signal from bubble collisions peaks at $k_p \sim \beta$, the inverse duration of the phase transition, the peak of the MHD signal is related to the bubble size: the peak wavelength becomes therefore $\lambda_p \sim R_* \simeq v/\beta$. The analysis of Ref. [41] finds a peak at about $k_p \sim \pi^2 \beta/v$. We can fit the GW spectrum obtained in [41] by the following formula:

MHD turbulence:

$$\frac{d\Omega_{\text{GW}}^{(\text{MHD})} h^2}{d\log k} \simeq \frac{8}{\pi^6} h^2 \Omega_{r0} \frac{\mathcal{H}_*}{\beta} \Omega_{S^*}^{3/2} v^4 \times \frac{(k/\beta)^3}{(1 + 4k/\mathcal{H}_*) [1 + (v/\pi^2)(k/\beta)]^{11/3}}. \quad (4)$$

For large scales, $k \ll k_p$, both spectra in Eqs. (3) and (4) increase as k^3 : this behavior is simply due to causality [37, 43]. Since the anisotropic stresses are generated by a causal process, their spectrum is white noise at scales larger than the typical correlation scale of the source, which corresponds to the bubble size. The white noise spectrum is inherited by the GWs: $\langle |\dot{h}|^2 \rangle \propto \text{const.}$, so that the GW energy density scales simply with the phase space volume k^3 . The behavior on small scales, $k \gg k_p$, depends on the source power spectrum and on the unequal time correlation properties of the source, see Ref. [44]. In particular, the result of Eq. (3) resides on the assumption that the bubbles are infinitely thin: this assumption holds if the bubbles propagate as detonations and causes the k^{-1} slope at high wave-numbers [31, 33]. On the other hand, the $k^{-5/3}$ decay of Eq. (4) is a consequence of the Kolmogorov type spectrum assumed for the MHD turbulent motions at high wave-numbers. In addition, the slope of the MHD signal changes at sub-horizon scales, $\mathcal{H}_* < k < k_p$, from k^3 to k^2 due to the long duration of the source (c.f. [41]).

From the the above formulas for the GW spectra we see that the basic ingredients which determine the peak position and amplitude are simply the fractional energy density of the source Ω_{S^*} , the duration of the phase transition β^{-1} , and the bubble velocity v (besides obviously the temperature at which the phase transition occurs T_* , which is parameterized by the Hubble scale \mathcal{H}_*). Ω_{S^*} and v are related, in a way which depends on the characteristics of the phase transition: for example its strength, the properties of the bubble expansion, the

interactions of the fluid particles with the field which is undergoing the transition, and so on. In early works on GWs from bubble collisions, it has been assumed that the bubbles expand as a Jouguet detonation, because in this case the above parameters can be calculated quite straightforwardly [27]. However, the recent analysis of [45] demonstrates that there is no particularly justified reason for this assumption, and other kinds of solutions for the bubble expansion are possible, such as deflagrations, runaway solutions and hybrids. Ref. [45] presents a model-independent description of the different regimes characterizing the bubble expansion, including the effect of friction due to the interaction of the bubble wall with the fluid particles. From a given particle physics model, one can in principle evaluate the friction parameter η and the strength of the phase transition $\alpha = \rho_{\text{vac}}/\rho_{\text{rad}}$. Once these two quantities are known, Ref. [45] provides a way to determine the bubble wall velocity v and the fraction of vacuum energy density which goes into kinetic energy of the bubble walls, $\kappa = \rho_{\text{kin}}/\rho_{\text{vac}}$. In terms of the parameter κ , the fractional source energy density for bubbles becomes

$$\Omega_{S^*}^{(\text{B})} = \kappa \frac{\alpha}{\alpha + 1}.$$

In the case of MHD turbulence, one further has to convert a part of the bubble wall kinetic energy to turbulence and magnetic fields. The efficiency of this conversion is not straightforward to estimate. Ref. [45] provides a relation between the bubble wall velocity and the fluid velocity at the bubble wall position v_f : in the most optimistic case, one can argue that the overall kinetic energy in turbulence is simply determined by this fluid velocity. In this case one would have $\Omega_{S^*}^{(\text{MHD})} \sim v_f^2/2$.

In the absence of a way to determine α and η from a given particle physics model, in the present analysis we have decided to keep the parameters completely model-independent. We make the simple assumption of equipartition, namely we assume the same energy density in colliding bubble walls and in MHD turbulence, $\Omega_{S^*}^{(\text{B})} = \Omega_{S^*}^{(\text{MHD})}$. This is more a reflection of our ignorance of how this energy density will be distributed than a well justified assumption; nevertheless, it seems to be a reasonable expectation and in the absence of a model for the phase transition it is the most straightforward assumption. We also assume a strongly first order phase transition, which induces super-sonic bubble velocities, $v > c_s$. We set the temperature of the QCD phase transition at $T_* = 100$ MeV. The other parameter relevant for the GW spectra is the duration of the phase transition, parametrised by β . In the electroweak case, this is usually taken to be (1–10)% of a Hubble time: $\beta = (10 - 100)\mathcal{H}_*$. This value is based on the estimate given in Ref. [21], which shows that β is related to the temperature of the phase transition through $\beta/\mathcal{H}_* \sim 4 \ln(m_{\text{P1}}/T_*)$, for a phase transition nucleated via thermal fluctuations. In the absence of a precise model for the QCD phase transition, in this section we

have decided to take $\beta = 10\mathcal{H}_*$, which is more favorable for observations with pulsar timing experiments. The analysis of [21] demonstrates that models of phase transitions with small values of β/\mathcal{H}_* may be rather exceptional, but cannot be ruled out by general arguments. The important point is that β/\mathcal{H}_* must be larger than unity, otherwise the phase transition is not fast with respect to the universe expansion and our assumptions no longer hold.

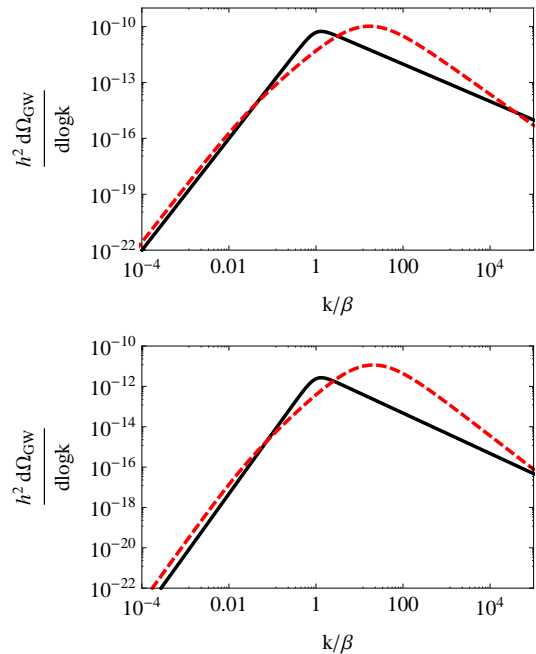


FIG. 1: The GW spectra from bubble collisions (black, solid) and from MHD turbulence (red, dashed) are shown for different values of $\Omega_{S^*} = 0.1$ and $v = 0.7$ (top panel) and $\Omega_{S^*} = 0.03$ and $v = 0.57 \simeq c_s$ (bottom panel). We set $\beta = 10\mathcal{H}_*$ and $T_* = 100$ MeV throughout.

In Fig. 1 we show the GW spectrum for both, bubbles and MHD turbulence for two different choices of the parameters Ω_{S^*} and v . The MHD turbulence signal dominates almost in the entire frequency range. At large scales, it is slightly higher due to the long duration of the turbulent source with respect to bubble collisions [41]. As already mentioned, the long duration of the source also causes the slope of the MHD signal to change at sub-horizon scales from k^3 to k^2 : consequently, for $\beta > k > \mathcal{H}_*$, i.e. $0.1 < k/\beta < 1$, the bubble collision signal prevails. This is valid up to the peak of the bubble collision signal, which arises before the turbulent one: at $k/\beta \simeq 1$, corresponding to the inverse characteristic time of the source, while the turbulent spectrum peaks at $k/\beta \simeq \pi^2/v$, corresponding to the inverse characteristic scale of the source. This causes the turbulent signal to dominate at interesting frequencies, since the total spectrum continues to raise after $k/\beta \simeq 1$ (only if the energy in turbulence is about one order of magnitude smaller than the one in bubble collisions, the collision

signal will dominate: however, this seems somewhat unnatural given the extremely high Reynolds number of the primordial fluid, and we discard this possibility in this work) [58].

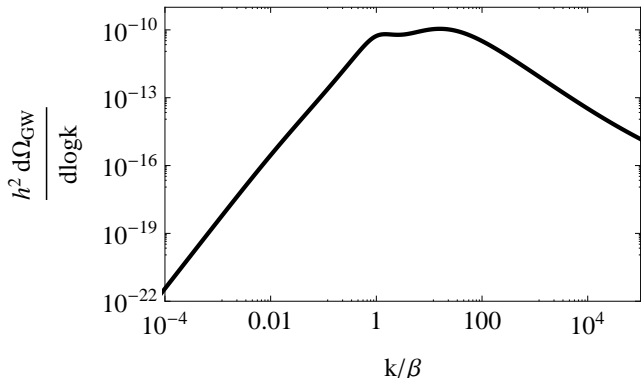


FIG. 2: The GW signal from bubble collisions and MHD turbulence for $\Omega_{S^*} = 0.1$ and $v = 0.7$. We choose $\beta = 10 \mathcal{H}_*$. The signal is dominated by the contribution from MHD turbulence. The bubble collision peak causes the hump on the left of the true peak of the spectrum.

In Fig. 2 we show the total signal for the more optimistic case, $\Omega_{S^*} = 0.1$ and $v = 0.7$. The peak frequency of the total GW spectrum corresponds to the MHD turbulence peak: $k/\beta \simeq \pi^2/v$, and depends on the choice $\beta = 10 \mathcal{H}_*$. From $f = k/(2\pi)$ one obtains [42, 44]

$$f_p \simeq 1.7 \cdot 10^{-9} \frac{\pi^2}{v} \frac{\beta}{\mathcal{H}_*} \left(\frac{g_*}{10}\right)^{\frac{1}{6}} \frac{T_*}{100 \text{ MeV}} \text{ Hz} \quad (5)$$

where g_* is the number of effective relativistic degrees of freedom at the temperature T_* . With $v = 0.7$, $\beta = 10 \mathcal{H}_*$, $g_* = 10$ and $T_* = 100 \text{ MeV}$ the peak frequency becomes $f_p \simeq 2.5 \cdot 10^{-7} \text{ Hz}$.

III. THE PULSAR TIMING ARRAY

Neutron stars can emit powerful beams of electromagnetic waves from their magnetic poles. As the stars rotate the beams sweep through space like the beacon of a lighthouse. If the Earth lies within the sweep of a neutron star's beams, the star is observed as a point source in space emitting short, rapid pulses of electromagnetic waves, and is referred to as a pulsar.

The electromagnetic pulses we observe arrive at a very steady rate due to the enormous moment of inertia of neutron stars. The idea to use these stable clocks to detect GWs was first put forward in the late 1970s [47–49]. Fluctuations in the time of arrival of pulses, after all known effects are subtracted, could be due to the presence of GWs. Recently pulsar timing precision has improved dramatically. Jenet and collaborators [50] have shown that the presence of nano-Hertz GWs could be detected using a pulsar timing array (PTA) consisting

of 20 pulsars with timing precisions of 100 nanoseconds over a period of 5 to 10 years (see also [4, 5] for more recent PTA sensitivity estimates). Pulsar timing arrays are most sensitive in the band $10^{-9} \text{ Hz} < f < 10^{-7} \text{ Hz}$. The lower limit in frequency is given by the duration of the experiment ($\sim 10 \text{ yr.}$) and the upper limit by the sampling theorem, i.e. the time between observations ($\sim 1 \text{ month}$). The spike in the sensitivity at $f = 0.3 \times 10^{-7} \text{ Hz}$ seen in Fig. 3 is the frequency of the earth's rotation around the sun which cannot be disentangled from a GW with the same frequency.

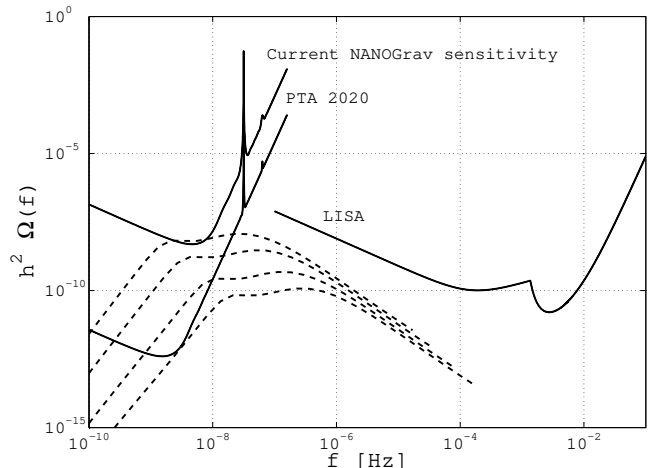


FIG. 3: Comparison of the GW spectrum $h^2 \Omega(f)$ with current NANOGrav pulsar timing array sensitivity and expected sensitivity of pulsar timing experiments in 2020 [5]. We have used $h = 0.73$, $\Omega_{r0} = 8.5 \times 10^{-5}$, $\Omega_{S^*} = 0.1$ and $v = 0.7$. We plot the GW spectra for the values $\mathcal{H}_*/\beta = 1, 0.5, 0.2, 0.1$ (dashed lines from top to bottom). For $\mathcal{H}_*/\beta \sim 1$, the background of GWs can just be detected in present pulsar timing experiments, while for $0.1 \lesssim \mathcal{H}_*/\beta$ it can be detected by the planned array IPTA2020 (very high values of $\mathcal{H}_*/\beta \sim 1$ are difficult to accommodate in the case of a thermally nucleated phase transition, c.f. discussion in the text). We also show the LISA sensitivity [52, 53]. Unfortunately, LISA will not be able to detect a signal from a first order QCD phase transition (the EW phase transition is more promising in this respect [25–41, 44, 46]).

The North American Nanohertz Observatory for Gravitational Waves (NANOGrav) [51], a collaboration of astronomers, has created a pulsar timing array—a galactic scale GW observatory using about 20 pulsars. It is a section of the IPTA, an international collaboration involving similar organizations of European and Australian astronomers. The current NANOGrav pulsar timing array sensitivity is shown in Fig. 3, together with the GW spectra we expect from the QCD phase transition as a function of frequency

$$h^2 \Omega_{\text{GW}}(f) = h^2 \frac{d\Omega_{\text{GW}}}{d\log k}, \quad (6)$$

for $\mathcal{H}_*/\beta = 1$ (top dashed line), $\mathcal{H}_*/\beta = 0.5$ (upper-

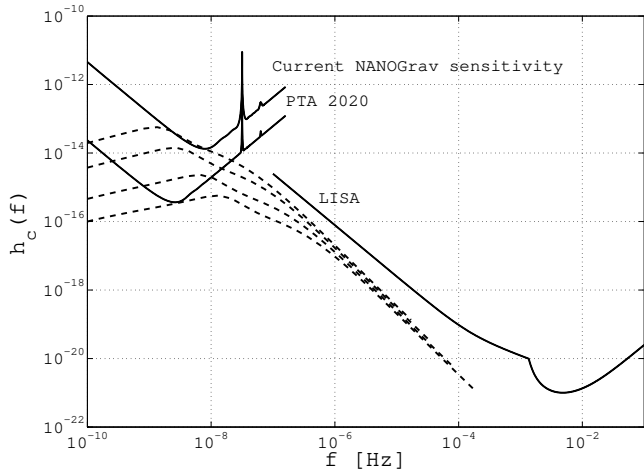


FIG. 4: Same as Fig. 3 but comparing the characteristic strain h_c as given by Eq. (7).

middle dashed line), $\mathcal{H}_*/\beta = 0.2$ (lower-middle dashed line), $\mathcal{H}_*/\beta = 0.1$ (bottom dashed line). We have used $h = 0.73$, $\Omega_{r0} = 8.5 \times 10^{-5}$ (which includes photons and neutrinos), $\Omega_{S*} = 0.1$ and $v = 0.7$. We have taken the frequency to be (c.f. Eq. (5))

$$f = 1.7 \times 10^{-9} \left(\frac{\beta}{\mathcal{H}_*} \right) \left(\frac{k}{\beta} \right) \text{ Hz}$$

i.e. chosen $T_* = 100 \text{ MeV}$, $g_* = 10$, and k/β varying between 10^{-4} and 10^4 (like in Figs 1 and 2). The signal is compared with the current sensitivity of the NANOGrav pulsar timing array, and the expected sensitivity of the IPTA pulsar timing array in 2020 [5]. For values of $0.1 \lesssim \mathcal{H}_*/\beta \lesssim 1$, the background of GWs would be detected with future pulsar timing array sensitivities. The value of \mathcal{H}_*/β must certainly be smaller than unity for the phase transition to be fast with respect to the Hubble time and for our approximations to apply. In most cases, if the phase transition happens at a temperature much smaller than the Planck temperature, \mathcal{H}_*/β is of the order of 0.01; however, higher values of this parameter cannot be excluded, and we adopt them here since they are more promising for detection [21].

Fig. 3 also shows the sensitivity of the planned Laser Interferometer Space Antenna (LISA) [52] assuming that some of the confusion noise from white dwarf binaries can be subtracted out [53]. LISA will not be able to detect the GW signature of a first order QCD phase transition: in order to be detectable by LISA, the GW spectrum must peak at higher frequency and consequently the phase transition must occur at higher temperature. LISA can in principle detect GWs from a strongly first order

EW phase transition at $T_* \simeq 100 \text{ GeV}$ [25–41, 44, 46, 54].

A related quantity often used in the pulsar timing community is the (dimensionless) characteristic strain, defined by [55]

$$h_c^2(f) = \frac{3H_0^2}{2\pi^2} f^{-2} \Omega_{\text{GW}}(f). \quad (7)$$

In Fig. 4 we show the same data as in Fig. 3 but in terms of the characteristic strain h_c .

IV. CONCLUSION AND OUTLOOK

A stochastic background of GWs from the QCD phase transition could be detected by pulsar timing experiments if the transition is strongly first order and lasts sufficiently long with respect to the Hubble time. In standard cosmology the QCD phase transition is not even second order, but simply a cross-over and in this case we do not expect it to generate GWs. However, if the neutrino chemical potential is sufficiently large [18], the QCD phase transition does become first order. The required chemical potential does not violate nucleosynthesis constraints, and if a sterile neutrino is the dark matter, we do actually expect a large neutrino chemical potential [19].

Pulsar timing experiments will reach unprecedented sensitivities in the next few years, and may open a new window on cosmology. The detection of a stochastic background with pulsar timing experiments could help to study the nature of the QCD phase transition, its duration, its strength and so on; by comparison with lattice calculations, this would allow us to determine the neutrino chemical potential and other properties of the so elusive cosmological neutrino sector. Furthermore, the amplitude and peak frequency of the spectrum are sensitive to the expansion rate of the Universe at this temperature [20], which remains unconstrained to date.

A first order QCD phase transition generating a GW background would also induce a stochastic background of magnetic fields, as studied in the past [56]. Furthermore, the GW background might have non-vanishing helicity, which would be an interesting phenomenon to investigate by itself [57].

Acknowledgments

We would like to thank Paul Demorest, Andrea Lomen, Larry Price and Geraldine Servant for useful conversations. RD acknowledges support from the Swiss National Science Foundation. XS is supported in part by NSF Grant No. PHY-0758155 and the Research Growth Initiative at the University of Wisconsin-Milwaukee.

[1] A. Einstein, Königlich Preussische Akademie der Wissenschaften, Sitzungsberichte, 688–696 (1916);

reprinted in: *Collected papers of A. Einstein*, A.J. Knox,

- J. Klein and R. Schulmann, eds., Vol. 6, 347, Princeton University Press (1996).
- [2] A. Lazzarini, R. Weiss (1996), LIGO technical report, LIGO-E950018-02; A. Abramovici, et al. *Science* **256**, 325 (1992); <http://www.ligo.caltech.edu/>.
- [3] F. Acernese et al., *Optics and Lasers in Engineering* **45**, 478-487, (2007); <http://www.virgo.infn.it/>.
- [4] G. Hobbs *et al.*, *Class. Quant. Grav.* **27**, 084013 (2010).
- [5] P. Demorest, J. Lazio, A. Lommen for the NANOGrav collaboration, arXiv:0902.2968 [astro-ph.CO].
- [6] J. S. B. Wyithe and A. Loeb, *Astrophys. J.* **590**, 691 (2003).
- [7] A. H. Jaffe and D. C. Backer, *Astrophys. J.* **583**, 616 (2003).
- [8] M. Enoki, K. T. Inoue, M. Nagashima, and N. Sugiyama, *Astrophys. J.* **615**, 19 (2004).
- [9] M. Kramer, D. C. Backer, J. M. Cordes, T. J. W. Lazio, B. W. Stappers, and S. Johnston, *New Astron. Rev.* **48**, 993 (2004).
- [10] A. Sesana, A. Vecchio, and C.N. Colacino, arXiv:0804.4476v2 [astro-ph] (2008).
- [11] A. Sesana and A. Vecchio, *Phys. Rev. D* **81**, 104008 (2010).
- [12] T. Damour and A. Vilenkin, *Phys. Rev. Lett.* **85**, 3761 (2000).
- [13] T. Damour and A. Vilenkin, *Phys. Rev. D* **64**, 064008 (2001).
- [14] T. Damour and A. Vilenkin, *Phys. Rev. D* **71**, 063510 (2005).
- [15] X. Siemens, V. Mandic, and J. Creighton, *Phys. Rev. Lett.* **98**, 111101 (2007).
- [16] S. Olmez, V. Mandic and X. Siemens, *Phys. Rev. D* **81**, 104028 (2010).
- [17] E. Witten, *Phys. Rev. D* **30**, 272 (1984).
- [18] D. Schwarz and M. Stuke, *JCAP* **11**, 025 (2009) [arXiv:0906.3434].
- [19] A. Boyarsky, O. Ruchaysliy and M. Shaposhnikov, *Ann. Rev. Nucl. Part. Sci.* **59** 191 (2009) [arXiv:0901.0011].
- [20] D. Chung and P. Zhou [arXiv:1003.2462] (2010).
- [21] C.J. Hogan, *Phys. Lett. B* **133**, 172 (1983).
- [22] C.J. Hogan, *MNRAS* **218**, 629 (1986).
- [23] M.S. Turner and F. Wilczek, *Phys. Rev. Lett.* **65**, 3080 (1990).
- [24] M.S. Turner, E.J. Weinberg and L.M. Widrow, *Phys. Rev. D* **46**, 2384 (1992).
- [25] A. Kosowsky, M.S. Turner and R. Watkins, *Phys. Rev. D* **45**, 4514 (1992).
- [26] A. Kosowsky and M.S. Turner, *Phys. Rev. D* **47**, 4372 (1993).
- [27] M. Kamionkowski, A. Kosowski and M.S. Turner, *Phys. Rev. D* **49**, 2837 (1994).
- [28] R. Acreda, M. Maggiore, A. Nicolis and A. Riotto, *Class. Quant. Grav.* **18**, L155 (2001).
- [29] R. Acreda, M. Maggiore, A. Nicolis and A. Riotto, *Nucl. Phys. B* **631**, 342 (2002).
- [30] S. Huber and T. Konstandin, *JCAP* **0805**, 017 (2008).
- [31] S. Huber and T. Konstandin, *JCAP* **0809**, 022 (2008).
- [32] C. Caprini, R. Durrer and G. Servant, *Phys. Rev. D* **77**, 124015 (2008).
- [33] C. Caprini, R. Durrer, T. Konstandin and G. Servant, *Phys. Rev. D* **79**, 083519 (2009).
- [34] C.J. Hogan, *Phys. Rev. Lett.* **51**, 1488 (1983).
- [35] A. Kosowsky, A. Mack and T. Kahniashvili, *Phys. Rev. D* **66**, 024030 (2002).
- [36] A.D. Dolgov, D. Grasso and A. Nicolis, *Phys. Rev. D* **66**, 103505 (2002).
- [37] C. Caprini and R. Durrer, *Phys. Rev. D* **74**, 063521 (2006).
- [38] G. Gogoberidze, T. Kahniashvili and A. Kosowsky, *Phys. Rev. D* **76**, 083002 (2007).
- [39] T. Kahniashvili, G. Gogoberidze and B. Ratra, *Phys. Rev. Lett.* **100**, 0231301 (2008).
- [40] T. Kahniashvili, L. Campanelli, G. Gogoberidze, Y. Maravin and B. Ratra, *Phys. Rev. D* **78**, 123006 (2008).
- [41] C. Caprini, R. Durrer and G. Servant, *JCAP* **0912**, 024 (2009) [arXiv:0909.0622].
- [42] R. Durrer, *The Cosmic Microwave Background*, Cambridge University Press (2008).
- [43] R. Durrer and C. Caprini, *JCAP* **0311**, 010 (2003). [arXiv:astro-ph/0305059].
- [44] R. Durrer, *J. Phys.: Conf. Ser.* **222** 012021, Proceedings of the 1st Mediterranean Conference on Classical and Quantum Gravity (MCCQG) [arXiv:1002.1389].
- [45] J. R. Espinosa, T. Konstandin, J. M. No, G. Servant, [arXiv:1004.4187].
- [46] A. Nicolis, *Class. Quant. Grav.* **21**, L27 (2004).
- [47] M. V. Sazhin, *Sov. Astron.* **22**, 36 (1978).
- [48] S. Detweiler, *Astrophys. J.* **234**, 1100 (1979).
- [49] D.R. Lorimer and M. Kramer, *Handbook of Pulsar Astronomy*, Cambridge University Press (2005).
- [50] F. A. Jenet, G. B. Hobbs, K. J. Lee, and R. N. Manchester, *Astrophys. J.* **625** L123, (2005).
- [51] <http://nanograv.org/>.
- [52] P. L. Bender, K. Danzmann, and the LISA Study Team, MPQ233 (1998); <http://lisa.nasa.gov/>.
- [53] S. A. Hughes, *Mon. Not. R. Astron. Soc.* **331**, 805–816 (2002).
- [54] A. Ashoorioon and T. Konstandin, *JHEP* **0907**, 086 (2009).
- [55] M. Maggiore, *Phys. Rept.* **331**, 283 (2000).
- [56] J. M. Quashnock et al, *Astrophys. J.* **344** (1989) L49; B. Cheng and A.V. Olinto, *Phys. Rev. D* **50** (1994) 2412; G. Baym et al., *Phys. Rev. D* **53** (1996) 662; M. McNeil Forbes, A.R. Zhitnitsky, *Phys. Rev. Lett.* **85**, 5268 (2000)[arXiv:hep-ph/0004051]; T. Boeckel and J. Schaffner-Bielich, arXiv:0906.4520[astro-ph.CO].
- [57] C. Caprini, R. Durrer and E. Fenu, *JCAP* **0911**, 001 (2009) [arXiv:0906.4976].
- [58] Contrary to Ref. [46], we find that the expected peak frequency of the GW spectrum from bubble collisions is always smaller than the one from MHD turbulence, the former being related to the duration of the phase transition while the latter to the size of the bubbles. This discrepancy arises because Ref. [46] assumed that the peak frequency for the GW spectrum from MHD turbulence is related to the turbulent eddy turnover time, while in our case it is determined by the time correlation properties of the GW source, as explained in details in Ref. [41].

This figure "qcdPTAandLISA.jpg" is available in "jpg" format from:

<http://arxiv.org/ps/1007.1218v3>